

describe the oxygen content of the original embryos and planetesimals as a function of their heliocentric distances of origin. Elements currently used for fitting are Fe, Si, O, Ni, Co, Nb, Cr, Ta and V. We concentrate here on the Grand Tack simulation SA154_767 in which starting planetesimals were distributed between 0.7 and 13 AU. This simulation produced four final planets including an approximately Earth-mass planet at 1 AU and an outer Mars-mass planet at 1.68 AU.

Results: In order to investigate the broadest possible parameter space, we consider three possible composition-distance models for the starting bodies. (1) Oxygen content is constant as a function of heliocentric distance, which is the requirement for homogeneous accretion. (2) Bodies that originate close to the Sun are oxidised and those originating further out are relatively reduced. (3) Bodies that originate close to the Sun are reduced and those originating further out are relatively-oxidised. In the case of models (1) and (2), it is not possible to create an Earth-like planet with a mantle composition close to that of the Earth's mantle and reduced chi squared values in the range 70-80 are obtained for the best fits. Model (3), on the other hand, results in excellent fits for all elements, giving reduced chi squared values in the range 1.5 – 3.0 with metal-silicate equilibration pressures ~60% of core-mantle boundary pressures. In addition, in marked contrast to models (1) and (2) a realistic Martian mantle FeO content of 18-20 wt% is obtained. However, it is not possible to define a unique composition-distance model in category (3). Two variations, which give equally good results, are shown in Fig. 1. In both cases, all Fe is initially present as metal in reduced compositions. In addition, up to 20% of available Si is initially dissolved in the metal – which further reduces the oxygen content. Fig. 1a shows a “step” model in which compositions beyond 1.7 AU are partially oxidized whereas Fig. 1b shows a “gradient” model in which compositions become increasingly oxidized between 1.2 and 3.1 AU and are fully oxidized beyond 3.1 AU.

Composition-distance models, such as those shown in Fig. 1, can be justified as follows. Oxygen fugacities of a solar gas are orders of magnitude more reducing than the intrinsic oxygen fugacities at which the terrestrial planets and meteorite parent bodies formed but are consistent with the region of highly-reduced compositions at <1-1.5 AU shown in Fig. 1. Thus extensive oxidation must have occurred in the early solar system with oxidation of Fe to form an FeO component in silicates being the major consequence. The most likely oxidant was water. The oxidation gradient shown in Fig. 1b can be explained as follows: Due to the net inflow of material in the solar nebula, ice-covered dust moves inwards from beyond the snow

line. Inside the snow line, water ice sublimates, thus adding H₂O to the vapour phase. As temperatures continue to rise and material continues to move inwards, H₂O-rich vapour reacts with Fe-bearing dust which results in oxidation. Inward still, vapour is H₂O-poor because the products of sublimated water ice have not mixed all the way to the innermost solar system. Here Fe remains free of oxidation and highly-reduced compositions are preserved.

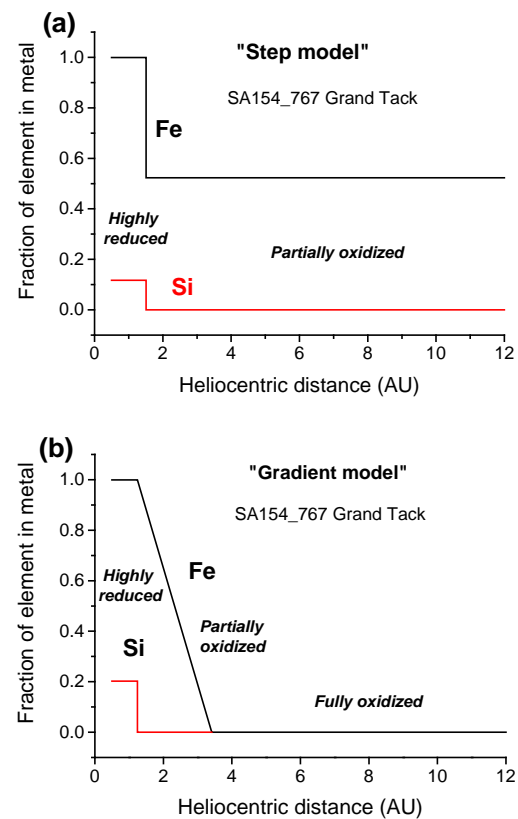


Figure 1. Two alternative composition-distance models that give equally good fits to the Earth's mantle composition in a combined N-body accretion simulation/multistage core formation model. In both cases, bodies in an inner region have highly reduced compositions with all Fe being present as metal and a significant proportion of available Si being dissolved in metal. Beyond 1-1.5 AU, compositions are more oxidised.

References: [1] O'Brien D. P. et al. (2006) *Icarus*, 184, 39-58. [2] Raymond S. N. et al. (2009) *Icarus*, 203, 644-662. [3] Walsh K. J. et al. (2011) *Nature*, 475, 206-209. [4] Rubie D. C. (2013) *EPSL*, 301, 31-42. [5] Frost D. J. (2010) *JGR*, 115, B02202. [6] Tonks W. B. and Melosh H. J. (1993) *JGR* 98,5319-5333. [7] Čuk M. and Stewart S. T. (2013) *Science* 338, 1047-1052. [8] Deguen R. et al. (2011) *EPSL* 310, 303-313.